

Structure and properties of oxygen-containing thin films and bulk MgB₂

T Prikhna^{1,6}, A Shapovalov¹, W Goldacker², M Eisterer³, A Kozyrev¹,
V Shaternik⁴, V Boutko⁵, A Gusev⁵, H W Weber³, M Karpets¹, T Basyuk¹,
V Sverdun¹, V Moshchil¹, M Belogolovskiy⁴ and N Sergienko¹

¹ V. Bakul Institute for Superhard Materials of the National Academy of Sciences of Ukraine, 2, Avtozavodskaya Str., Kiev 07074, Ukraine

² Karlsruhe Institute of Technology (KIT), 76344 Eggenstein, Germany

³ Atominstitut, Vienna University of Technology, Stadionallee 2, 1020 Vienna, Austria

⁴ G.V. Kurdyumov Institute for Metal Physics of the National Academy of Sciences of Ukraine, 03680 Kyiv, Ukraine

⁵ Donetsk Institute for Physics and Engineering named after O.O. Galkin of the National Academy of Sciences of Ukraine, R. Luxemburg str.72, Donetsk-114, 83114, Ukraine

E-mail: ¹ prikhna@mail.ru, ² wilfried.goldacker@kit.edu, ³ eisterer@mail2.ati.ac.at, ⁴ shaternik@mail.ru, ⁵ boutko@teor.fti.ac.donetsk.ua

Abstract. A structural Auger spectroscopy study of MgB₂ thin (~140 nm) oxygen-containing polycrystalline films produced by magnetron sputtering and 99% dense MgB₂ bulks synthesized at 2 GPa allows us to conclude that j_c of MgB₂ depends to a high extent on the amount and distribution of oxygen in the material matrix. j_c reached 7.8-2.7 MA/cm² below 1T at 20 K in the films and 0.3-0.9 MA/cm² (depending on the boron used) in the bulks. The higher j_c in MgB₂ thin films can be associated with finer oxygen-enriched Mg-B-O inclusions and their higher density in the film structure compared to the bulk. Calculations of the total electron density of states (DOS) in MgB₂, MgB_{1.75}O_{0.25}, MgB_{1.5}O_{0.5} and MgBO showed that all the compounds are conductors with metal-like behaviour. The DOS is even higher in MgB_{1.5}O_{0.5} than in MgB₂ and the binding energy is similar. So, the experimentally found presence of some dissolved oxygen in MgB₂ does not contradict its high SC performance. The introduction of a high amount of oxygen into the MgB₂ structure does not dramatically reduce the material's T_c and allows obtaining high j_c as observed in our MgB₂ films and bulks.

1. Introduction

Although MgB₂ is an oxygen-free superconductor, the high affinity of Mg toward oxygen makes it practically impossible to synthesize MgB₂-based materials free of oxygen. Eom et al. [1] established that in thin MgB₂ films (with a c-axis parameter of 0.3547 nm, which was larger than that for bulk material: 0.3521 nm) the substitution of oxygen for boron in the boron layers leads to a lower T_c but to a steeper slope of dH_{c2}/dT both in the parallel and perpendicular magnetic field than that for films with

⁶ To whom any correspondence should be addressed.



normal parameters. Also, the authors supposed that additional co-pinning by the non-superconducting MgO particles can contribute to the total pinning force. Birajdar et al. [2] found in MgB₂ grains of tapes oxygen-enriched regions and MgO precipitates of size 15–70 nm. The high O/Mg mole fraction ratio (0.23 for precipitates and 1.64 for an O-rich region) gave the authors of [2] reason to consider the precipitate as being MgO and the O-rich region being a mixture of MgO and Mg(OH)₂. Liao et al. [3, 4] using high-resolution transmission electron microscopy (HREM) have shown that the oxygen substitution occurs in the bulk of MgB₂ grains to form coherently ordered MgB_{2-x}O_x precipitates from about 5 up to 100 nm in size and that such precipitates can act as pinning centers, thus increasing the critical current density. These precipitates as assumed in [3, 4] were formed due to the ordered replacement of boron atoms by atoms of oxygen and are of the same basic structure as the MgB₂ matrix, but with composition modulations, and no difference in the lattice parameters between the precipitates and the matrix can be detected in conventional electron diffraction patterns. However, extra satellite diffraction spots were seen in some directions implying a structural modulation nature of the precipitates. The precipitates have the same orientation as the MgB₂ and the replacement of boron by oxygen makes the precipitates stronger in electron scattering. The periodicity of oxygen atom ordering depends on the concentration of oxygen atoms in the precipitate and first of all occurred in the (010) plane. A long-term exposure to oxygen at high temperatures results in the transformation of Mg(B₂O)₂ precipitates to MgO with a little change in precipitate sizes. The density of the precipitates of sizes 10–50 nm has been 10¹⁵/cm³, and of size 50–100 nm has been 10¹⁴/cm³ [4]. The unit cell structure of the inclusions essentially did not differ from that of the MgB₂, which, in parallel with the low X-ray atomic scattering factor of B, can be the explanation of the difference in results between X-ray and SEM-EDX examinations of MgB₂-based materials.

Our previous SEM–Auger study [5] showed that the MgB₂ matrix of the MgB₂ material synthesized from Mg:2B at 2 GPa with high j_c contained some dissolved admixture of oxygen, but much more admixture of oxygen was present in the separate oxygen-enriched inclusions (if synthesis temperature was about 900–1100 °C) or nanolayers (if the synthesis temperature was about 600–800 °C). So, it was concluded that the MgB₂ material consists of the MgB₂ phase (mainly) with small amount of dissolved oxygen and a MgO phase with dissolved boron. This can be the reason why in x-ray diffraction pattern just MgB₂ and MgO have been observed. The presence of higher magnesium borides MgB_x ($x > 4$), seen by SEM and shown by Auger analysis to have a very low oxygen content, was not possible to determine by x-ray due to their fine dispersion in the structure and the large number of low symmetry atoms in the unit cell what essentially reduce the intensities of the x-ray reflections as compared to those of the MgB₂.

The present study compared structure and properties of superconducting oxygen-contained MgB₂ bulk and thin-film materials in connection with calculated densities of states for pure MgB₂ and for compounds with different oxygen substitution for boron.

2. Experimental

The bulk MgB₂ materials were synthesized from Mg and B taken in the Mg:2B stoichiometry at high quasihydrostatic pressure (2 GPa) and 800 or 1050 °C for 1 h (in contact with BN). We used Mg turnings Technical Specification of Ukraine 48-10-93-88 and commercially available precursor B powders from HC Starck. We used two boron powders; boron-1 (designated as B-1) with a grain size <5 μm, 0.66 wt% O, 0.31 wt% C, 0.48 wt% N, and 0.32 wt% H; and boron-2 (designated as B-2) with a grain size of 4 μm, 1.5 wt% O, 0.47 wt% C, 0.40 wt% N, and 0.37 wt% H. Boron and magnesium were mixed and milled in a high-speed planetary activator with steel balls for 1–3 minutes.

The thin MgB₂ films were deposited by DC magnetron sputtering under 1 Pa Ar pressure on 8×8×0.2 mm³ sized (001) sapphire substrates at room temperature, which subsequently were annealed at 600–650 °C for 5 min in Ar under 10 Pa. For deposition we used a MgB₂ target synthesized by hot pressing at 30 MPa, 800 °C, 1 h using boron powder B-2.

The microstructure of the materials was characterized by x-ray structure analysis (with Rietveld refinement) and by SEM with microprobe x-ray and Auger (JAMP–9500F) analysis. The

Augerspectroscopy JAMP-9500F is combined in the same device with a high resolution SEM. It is possible to change the SEM microprobe analyzer for the Auger probe and perform etching of the $1 \times 1 \text{ mm}^2$ analyzed material surface area by Ar ions in the studies. JAMP-9500F offers the possibility to analyze quantitatively small volumes of about 10 nm in diameter and 1 nm in the depth. In situ etching can remove surface oxides that form between the time the sample is polished and analyzed, allowing pristine MgB_2 surfaces to be analyzed, as well as the composition of nano-inclusions and nano-layers.

The critical current density, j_c , was estimated from magnetization measurements in an Oxford Instruments 3001 vibrating sample magnetometer (VSM) using the Bean model. The connectivity was estimated from the difference in resistivity at 40 K and 300 K measured by the four probe technique. The amount of the superconducting (SC) shielding fraction was calculated from the ac susceptibility at 5 K with a numerical correction for the demagnetization of the actual sample geometry.

3. Results and discussions

The difference in SC behaviour of MgB_2 bulk materials depending on synthesis temperatures can be characterized as an increase of critical current densities j_c in low and medium magnetic fields with increasing synthesis temperature and an increase of j_c in high magnetic fields with decreasing synthesis temperature (see, for example, figure 1 a). Such behaviour has been observed for materials produced from different types of initial borons without and with additions such as Ti, Zr, Ta, SiC. The typical X-ray diffraction pattern of MgB_2 synthesized at 1050 °C using boron B-1 (sample I in table 1) is presented in figure 1b. Sample I showed the highest j_c at 20 K of 0.9 and 0.7 MA/cm², at 0 and 1 T respectively, see figure 1a). Sample I contains a well crystallized MgB_2 phase and admixing MgO and BN phases (Table 1). Sample II made with boron B-2, which contained more oxygen, was also made at 1050 °C, and contains the same phases (table 1), but the MgO concentration is higher. Sample II had j_c at 20 K of 0.4 and 0.3 MA/cm² at 0 and 1 T, respectively. It also had 99% density, 80% connectivity, and contained 94% of shielding fraction.

It should be mentioned that materials synthesized at lower temperature (800 °C) contain approximately the same amount of MgO as that prepared at 1050 °C using the same type of boron, but their structure contains some MgH_2 and unreacted Mg. The sizes of the inclusions of unreacted magnesium were rather big and the inclusions were randomly distributed so they cannot be effective pinning centers in MgB_2 . Thus synthesis temperature does not influence general oxygen concentration in MgB_2 , but oxygen impurities in the initial boron does.

The detailed study of MgB_2 structures by SEM and Auger showed that no MgO was found in the MgB_2 but Mg-B-O nanolayers "L" 10-20 nm thick ("L" is brightest regions in figure 1d) were found if material was synthesized under low temperature (800 °C). Such nanolayers had a stoichiometry near $\text{MgB}_{1.2-2.7}\text{O}_{1.8-2.5}$, as Auger quantitative analysis showed. In the materials synthesized at high temperature (1050 °C) segregation of oxygen occurred and in the MgB_2 matrix separate Mg-B-O inclusions "I" formed (which appear as the brightest regions in figure 1f and had

Table 1. Phases present in bulk MgB_2 (synthesized at 2 GPa, 1050 °C, 1 h using boron B-1 and B-2) and their lattice parameters.

| Sample I Mg:2B (boron B-1): 91 mass% (90 vol.%) MgB_2 , 5 mass% (5 vol.%) MgO, and 4 mass% (5 vol.%) BN | | | | |
|--|---------------|---------------|---------------|---------------|
| MgB_2 | | MgO | BN | |
| <i>a</i> , nm | <i>c</i> , nm | <i>a</i> , nm | <i>a</i> , nm | <i>c</i> , nm |
| 0.30844 | 0.35215 | 0.42227 | 0.25060 | 0.66830 |
| Sample II Mg:2B (boron B-2): 77 mass% (82 vol.%) MgB_2 , 13 mass% (10 vol.%) MgO and 10 mass% (8 vol.%) BN | | | | |
| MgB_2 | | MgO | BN | |
| <i>a</i> , nm | <i>c</i> , nm | <i>a</i> , nm | <i>a</i> , nm | <i>c</i> , nm |
| 0.30844 | 0.35236 | 0.42202 | 0.25040 | 0.66862 |

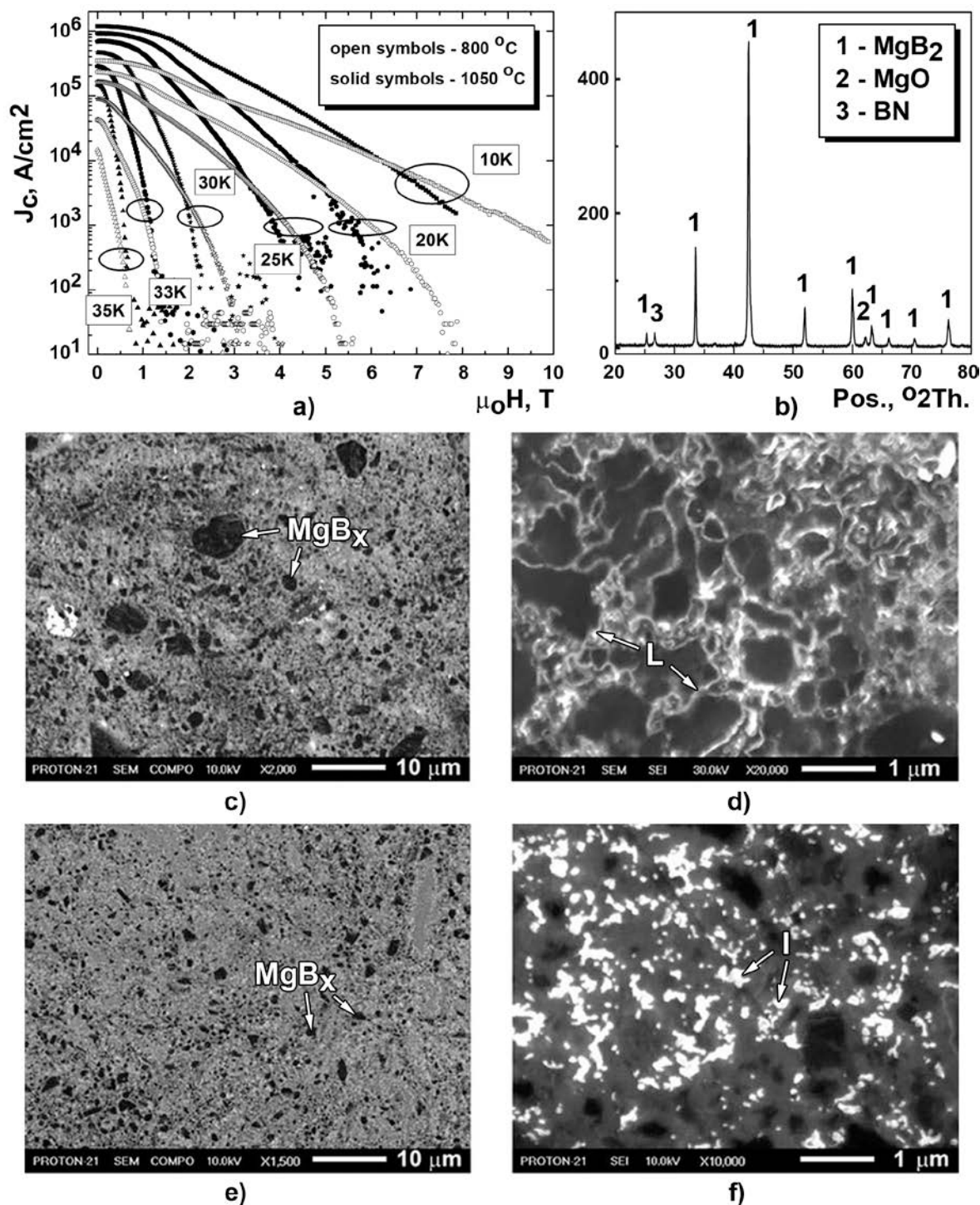


Figure 1. (a) - Critical current density, j_c , vs. magnetic field, $\mu_0 H$, at 10, 20, 25, 30, 33 and 35 K of bulk MgB₂ materials synthesized at 2 GPa for 1 h from Mg:2B(1) at 800 °C (open symbols) and 1050 °C (solid symbols); (b) - x-ray diffraction pattern of bulk MgB₂ synthesized at 2 GPa, 1050 °C for 1 h from B-1; (c-f) – structures (after surfaces etching by Ar) in BEI (c, e) and SEI (d, f) SEM modes of bulk MgB₂ samples prepared at 2 GPa, 1 h at 800 °C from B-1 (c, d) and 1050 °C from B-2 (e, f).

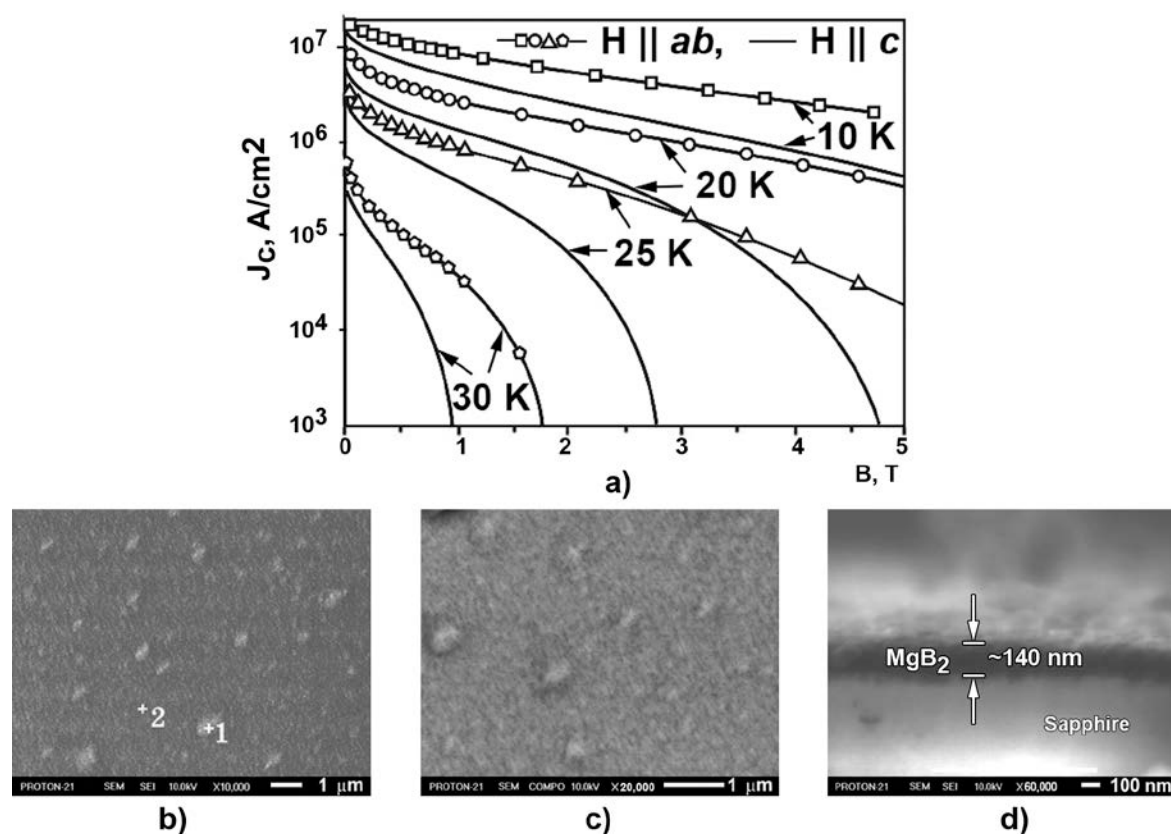


Figure 2. (a) - Critical current density, j_c , vs. magnetic field, B , at 10, 20, 25, 30, 33 and 35 K of thin MgB_2 film (for the cases when the field is parallel ($H||ab$ - lines with symbols) and perpendicular ($H||c$ - lines without symbols) to the substrate surface); (b-d) – structures (after surface etching by Ar) of MgB_2 film surface (b, c) and edge (d) in SEI (b, d) and BEI (c) SEM modes (oxygen enriched areas look brighter).

stoichiometry near $\text{MgB}_{0.6-0.8}\text{O}_{0.8-0.9}$). So, synthesis temperature can affect oxygen distribution in the MgB_2 structure. Besides this, a decrease of the sizes of inclusions of higher magnesium borides MgB_x ($x \approx 11-13$, which Auger analysis showed having stoichiometry near $\text{MgB}_{11-13}\text{O}_{0.2-0.3}$) takes place if the synthesis temperature increases (which are the darkest regions in figures 1c-f).

Auger spectra obtained from the MgB_2 matrix (appears grey) of the bulk sample presented in figure 1f showed stoichiometry near $\text{MgB}_{2.2-1.7}\text{O}_{0.4-0.6}$ from multiple analyses after multiple etching steps, which provided a depth profile. The quantitative Auger analysis allows an excellent localization of the electron beam and Ar etching in the chamber during analysis, so the oxidized layer that formed between the time the samples was polished and when it was analyzed was removed from the surface of the material before the analysis so the presence of oxygen in high amount in the “bright” nanolayers and inclusions as well as some small amount of oxygen in the MgB_2 matrix is from the sample synthesis. We cannot specify the exact stoichiometry of the oxygen-enriched layers or inclusions, but can determine that the relative amount of oxygen in their composition is high.

Figure 2 present j_c dependences (figure 2a) with the magnetic field in two perpendicular directions for the thin (140 ± 10 nm) MgB_2 film and the correlated SEM SEI (figure 2b, d) and BEI (figure 2c) images. The SEM images were taken in two perpendicular directions. j_c in the film at 20 K ranged from 7.8 to 2.7 MA/cm^2 for 0 and 1 T, respectively. Auger studies gave approximate compositions at points 1 and 2 in figure 2b of $\text{MgB}_{3.6}\text{O}_{2.4}\text{C}_{0.5}$ and $\text{MgB}_4\text{O}_{1.2}\text{C}_{0.8}$, respectively. Thus the brighter colour

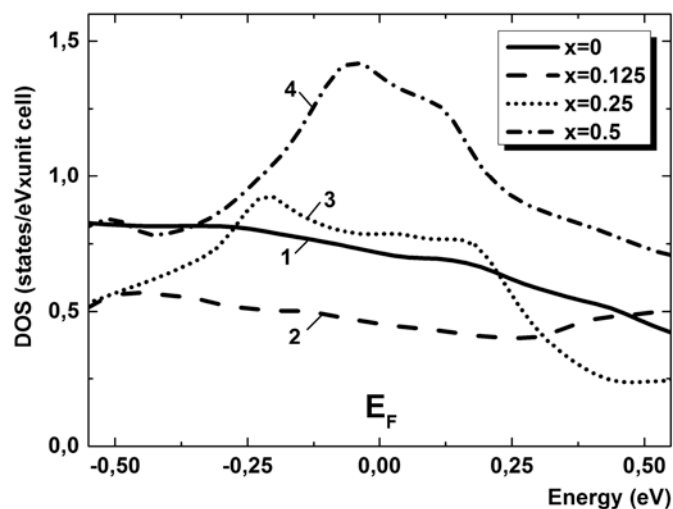


Figure 3. Calculated density of states (DOS) for MgB_2 (curve 1) and $\text{Mg}(\text{B}_{1-x}\text{O}_x)_2$: $\text{MgB}_{1.75}\text{O}_{0.25}$ (curve 2), $\text{MgB}_{1.5}\text{O}_{0.5}$ (curve 3) and MgBO (curve 4).

appears mainly due to a higher oxygen concentration (approximately two times) and figure 2c demonstrates the presence in the thin film of a high density of very fine oxygen-enriched inhomogeneities. The Auger quantitative analysis is very sensitive to the presence of light elements and for a correct quantitative estimation a reference spectrum should be used for the respective compound, which is not available, even for MgB_2 . So, the present estimations were done using reference spectra of other boron-, magnesium-, oxygen- and carbon-containing substances. Because of this we do not know the exact stoichiometry, but using the same reference spectra we can estimate to what extent the relative amount of each element in the material. It should be mentioned that oxygen-enriched inhomogeneities marked by “1” in figure 2b appeared due to non-uniform evaporation of magnesium (because of eruption of big Mg clusters) and these cannot be the relevant pinning centers due to their rather big size and sparse distribution. The pinning can be due to the smaller, “bright” oxygen-enriched nano-inclusions, the density of which in the material is extremely high (figure 2c).

Figure 3 presents calculated total density of electronic states in $\text{Mg}(\text{B}_{1-x}\text{O}_x)_2$ compounds: pure MgB_2 , $\text{MgB}_{1.75}\text{O}_{0.25}$, $\text{MgB}_{1.5}\text{O}_{0.5}$ and MgBO . To analyze the Mg-B-O compounds, we have applied the density functional theory [6] based on a full-potential linearized augmented plane wave method with the generalized gradient correction to exchange-correlation potential [7] using WIEN2k [8]. In the nearest vicinity of the Fermi energy E_F corresponding dependencies are not constant (figure 3) and their changes with x are non-monotonous. But, in any case, all studied compounds are conductors with a non-zero density of states at the Fermi level. Large density of delocalized states proves the metallic type of charge transport in them. Table 2 compares the total densities of states and related binding energies E_b in the studied Mg-B-O compounds. The numerical study of possible lattice distortion effects in the oxygen-enriched compounds showed that, for $x = 0.125$ and 0.25 , deviations from the unperturbed lattice are indeed small, while it is not so for $x = 0.5$. In our opinion, this indicates the presence of an upper metastable boundary for the Mg-B-O system when the oxygen content increases. It should be noted that a rise of DOS near Fermi level with oxygen doping $x \geq 0.25$ (figure 3) increases the total energy (table 2) and can be therefore energetically unfavourable. A comparison of E_b shows that the appearance of $\text{Mg}(\text{B}_{1-x}\text{O}_x)_2$ with hexagonal symmetry in the case of comparatively low oxygen content ($x \approx 0.25$) thus seems possible from this viewpoint. According to Auger estimation the superconductor had near $\text{MgB}_{2.2-1.7}\text{O}_{0.4-0.6}$ stoichiometry.

Table 2. Total DOSs and binding energies, E_b , in the $\text{Mg}(\text{B}_{1-x}\text{O}_x)_2$ compounds.

| x | 0 | 0.125 | 0.25 | 0.5 |
|------------|------|-------|------|------|
| total DOS | 0.72 | 0.43 | 0.96 | 1.36 |
| E_b , Ry | 1.12 | 1.10 | 1.06 | 0.94 |

The concentrations of oxygen in the Mg-B-O inclusions (“T”) and nanolayers (“L”) in bulk MgB_2 (figure 1d, f) are rather high and most probably they have a structure which is close to MgO (solid solution of boron in MgO) and they can thus be effective pinning centres. The formation of nanostructural inhomogeneities with different oxygen content in magnesium diboride seems to be one of the main factors for improving the transport characteristics in MgB_2 and the presence of some oxygen in the MgB_2 matrix is not an obstacle for attaining high SC currents.

4. Conclusions

The comparison of nanostructures of MgB_2 oxygen-containing thin film (with thickness of ~ 140 nm) and highly dense oxygen-containing bulk materials (synthesized under 2 GPa pressure) demonstrating a high superconductive performance gave us reasons to conclude that the critical current density, j_c , of MgB_2 -based materials to a high extent depends on the distribution of admixture oxygen what can be regulated by manufacturing conditions and by the synthesis temperature, in particular. The higher j_c of MgB_2 thin films as compared to bulk was explained by the higher density of finer oxygen-enriched Mg-B-O inhomogeneities in the film structure. The results of calculations of the electron density of states in MgB_2 , $\text{MgB}_{1.75}\text{O}_{0.25}$, $\text{MgB}_{1.5}\text{O}_{0.5}$ and MgBO demonstrated that all the compounds are conductors with metal-like behavior. The stoichiometry of the matrix of bulk MgB_2 materials having high SC performance was about $\text{MgB}_{2.2-1.7}\text{O}_{0.4-0.6}$ (according to Auger quantitative analysis), i.e. very near to the composition $\text{MgB}_{1.5}\text{O}_{0.5}$ with one of the calculated low binding energies. The introduction of a high amount of oxygen into the MgB_2 material’s structure does not dramatically reduce the material’s T_c and allows obtaining a high j_c .

Acknowledgement

This work was in parts performed within the German-Ukrainian project HICONSU (FKZ: 01DK13031) supported by German Ministry of Education and Research (BMBF) and within Austrian-Ukrainian project UA 01/2015. The content and the results are the opinion of the authors.

References

- [1] Eom C B, Lee M K, Choi J H, Belenky L J, Song X, Cooley L D, Naus M T, Patnaik S, Jiang J, Rikel M, Polyanskii A, Gurevich A, Cai X Y, Bu S D, Babcock S E, Hellstrom E E, Larbalestier D C, Rogado N, Regan K A, Hayward M A, He T, Slusky J S, Inumaru K, Haas M K and Cava R J 2001 *Nature* **411** 558.
- [2] Birajdar B, Braccini V, Tumino A, Wenzel T, Eibl O and Grasso G 2006 *Supercond. Sci. Technol.* **19** 916
- [3] Liao X Z, Serquis A C, Zhu Y T, Huang J Y, Civale L, Peterson D E, Mueller F M and Xu H 2003 *Journal of Applied Physics* **93** 6208
- [4] Liao X Z, Serquis A, Zhu Y T, Huang J Y, Civale L, Peterson D E, Mueller F M, Xu H *F cond-mat/0212571*
- [5] Prikhna T A, Eisterer M, Weber H W, Gawalek W, Kovylaev V V, Karpets M V, Basyuk T.V. and Moshchil V E 2014 *Supercond. Sci. Technol.* **27**, No 4 044013
- [6] Parr R G and Yang W 1989 Density-Functional Theory of Atoms and Molecules, *Oxford Univ. Press*.
- [7] Perdew J P, Burke S and Ernzerhof M Phys. 1996 *Rev. Lett.* **77** 3865
- [8] Blaha P, Schwarz K, Madsen G K H, Kvasnicka D and Luitz J 2001 WIEN2K, An augmented plane wave + local orbitals program for calculating crystal properties. *Techn. Univ. Wien*.